Human tetraspanin CD81 facilitates invasion of Salmonella enterica into human epithelial cells

Kris Gerard Alvarez, Lisa Goral, Abdulhadi Suwandi, Lisa Lasswitz, Francisco Zapatero-Belinchón, Katrin Ehrhardt, Kumar Nagarathinam, Katrin Künnemann, Thomas Krey, Agnes Wiedemann, et al.

Virulence

ISSN: (Print) (Online) Journal homepage: www.tandfonline.com/journals/kvir20

Human tetraspanin CD81 facilitates invasion of *Salmonella enterica* into human epithelial cells

Kris Gerard Alvarez, Lisa Goral, Abdulhadi Suwandi, Lisa Lasswitz, Francisco J. Zapatero-Belinchón, Katrin Ehrhardt, Kumar Nagarathinam, Katrin Künnemann, Thomas Krey, Agnes Wiedemann, Gisa Gerold & Guntram A. Grassl

To cite this article: Kris Gerard Alvarez, Lisa Goral, Abdulhadi Suwandi, Lisa Lasswitz, Francisco J. Zapatero-Belinchón, Katrin Ehrhardt, Kumar Nagarathinam, Katrin Künnemann, Thomas Krey, Agnes Wiedemann, Gisa Gerold & Guntram A. Grassl (06 Sep 2024): Human tetraspanin CD81 facilitates invasion of *Salmonella enterica* into human epithelial cells, Virulence, DOI: 10.1080/21505594.2024.2399792

To link to this article: https://doi.org/10.1080/21505594.2024.2399792

Publisher: Taylor & Francis & Informa UK Limited, trading as Taylor & Francis Group

Journal: *Virulence*

DOI: 10.1080/21505594.2024.2399792

Human Tetraspanin CD81 facilitates invasion of *Salmonella enterica* into human epithelial cells

Kris Gerard Alvarez[1], Lisa Goral[1], Abdulhadi Suwandi[1,3], Lisa Lasswitz[4], Francisco J. Zapatero-Belinchón[4], Katrin Ehrhardt[1], Kumar Nagarathinam[5,6], Katrin Künnemann[1], Thomas Krey[5,6,7,8,9], Agnes Wiedemann[10], Gisa Gerold[4,11,12], Guntram A. Grassl[1,2]

1. Institute of Medical Microbiology and Hospital Epidemiology, Medizinische Hochschule Hannover, Germany
2. German Centre for Infection Research (DZIF), Partner site Hannover-Braunschweig, Hannover, Germany
3. Institute of Cell Biochemistry, Hannover Medical School, Hannover, Germany
4. Tierärztliche Hochschule Hannover, Department of Biochemistry & Research Center for Emerging Infections and Zoonoses (RIZ), Hannover, Germany
5. Institute for Biochemistry, Universität zu Lübeck, Lübeck Germany
6. Excellence Cluster 2155 RESIST, Medizinische Hochschule Hannover, Hannover, Germany.
7. Institute of Virology, Medizinische Hochschule Hannover, Hannover, Germany
8. German Centre for Infection Research (DZIF), partner site Hamburg-Lübeck-Borstel-Riems, Lübeck, Germany
9. Centre for Structural Systems Biology (CSSB), 22607 Hamburg, Germany
10. IRSD - Institut de Recherche en Santé Digestive, ENVT, INRAE, INSERM, Université de Toulouse, UPS, Toulouse, France
11. Department of Clinical Microbiology, Umeå University, Sweden
12. Wallenberg Centre for Molecular Medicine (WCMM), Umeå University, Sweden

Corresponding author

Guntram A. Grassl
Hannover Medical School
Institute of Medical Microbiology and Hospital Epidemiology
Carl-Neuberg-Str. 1
30625 Hannover
Germany
Telefon: +49 511 532 4540
Telefax: +49 511 532 4366
Email: grassl.guntram@mh-hannover.de

Abstract

Human CD81 and CD9 are members of the tetraspanin family of proteins characterized by a canonical structure of four transmembrane domains and two extracellular loop domains. Tetraspanins are known as molecular facilitators, which assemble and organize cell surface receptors and partner molecules forming clusters known as tetraspanin-enriched microdomains. They have been implicated to play various biological roles including an involvement in infections with microbial pathogens. Here, we demonstrate an important role of CD81 for the invasion of epithelial cells by *Salmonella enterica*. We show that overexpression of CD81 in HepG2 cells enhances invasion of various typhoidal and non-typhoidal *Salmonella* serovars. Deletion of CD81 by CRISPR/Cas9 in intestinal epithelial cells (C2BBe1 and HT29-MTX-E12) reduces *S.* Typhimurium invasion. In addition, the effect of human CD81 is species-specific as only human but not rat CD81 facilitates *Salmonella* invasion. Finally, immunofluorescence microscopy and proximity ligation assay revealed that both human tetraspanins CD81 and CD9 are recruited to the entry site of *S.* Typhimurium during invasion but not during adhesion to the host cell surface. Overall, we demonstrate that the human tetraspanin CD81 facilitates *Salmonella* invasion into epithelial host cells.

Keywords

Salmonella, intestinal epithelium, tetraspanins, infection, invasion

Introduction

Salmonella is a gram-negative, rod-shaped bacterium, which continues to be a major cause of bacterial enteric illness throughout the world. Nontyphoidal *Salmonella* frequently colonizes the gastrointestinal tracts of livestock and poultry and there are limited effective interventions for prevention of disease in humans. Salmonellosis is the second most common bacterial gastrointestinal infection in humans after campylobacteriosis and is a major cause of foodborne outbreaks [1]. Therefore, understanding the mechanisms that contribute to *Salmonella* infection of host cells is paramount for designing effective intervention strategies that can prevent or alleviate the burden of *Salmonella* infections.

Eukaryotic tetraspanins are defined by a common structure which is composed of four transmembrane domains with short cytosolic N- and C-terminal regions, and two extracellular loops termed short extracellular loop (SEL) and large extracellular loop (LEL) [2]. Tetraspanins interact with a diverse array of eukaryotic surface and cytosolic proteins through lateral organization and interaction at the cytoplasmic domains. Thus, they localize receptors and interacting partner proteins to a defined region on the cell surface, forming clusters of tetraspanins and associated proteins, termed "tetraspanin-enriched microdomains" (TEMs) [3]. By clustering receptor proteins locally, tetraspanins act as molecular scaffolds, amplifying cellular signaling processes and corresponding biological processes, such as cellular adhesion, motility, and membrane fusion [4].

In mammals, 33 tetraspanins have been described. CD81 has been extensively studied and the crystal structure of the full-length protein in complex with cholesterol is known [5]. Although the function of the CD81 SEL is yet to be fully elucidated, the LEL has five distinct helical segments and is postulated to be responsible for tetraspanin oligomerization [6]. Additionally, a cholesterol-binding pocket which was postulated to regulate an open-to-closed conformational switch of the tetraspanin and affect its molecular interactions with partner proteins, was deduced from molecular modelling studies and tested experimentally [5]. Moreover, the intracellular domains (intracellular loop and the N- and C-termini) are implicated to provide a link to intracellular signaling molecules [7].

In recent years, it has been demonstrated that entry into host cells of several pathogens including viruses [8], bacteria [9] and parasites [10] is tetraspanin-dependent. For example, CD81

plays a key role as receptor for hepatitis C virus (HCV) entry [11,12]. In addition, CD81 facilitates *Listeria monocytogenes* invasion in HeLa cells and macrophages [13,14], and CD81 and CD9 were shown to directly influence *Burkholderia pseudomallei* membrane fusion and facilitate bacterial spread [15]. Moreover, antibody blocking of tetraspanins such as CD63 was demonstrated to inhibit *Salmonella* binding but not bacterial uptake into human monocyte-derived macrophages [16].

Adhesion and invasion of the intestinal epithelium is a critical step for *Salmonella* to initiate infection. Salmonellae invade into epithelial cells by bacterial-mediated macropinocytosis, through either a trigger-mediated invasion (using a Type III secretion machinery) or via a zipper-like invasion mechanism (eg. via the outer membrane proteins Rck and PagN) [17,18]. After translocation across the epithelium, the bacteria can be taken up by macrophages and dendritic cells. Coupled with intestinal inflammatory reactions, these processes eventually result in diarrhea and intestinal inflammation. Here, we demonstrate that human CD81 species-specifically supports invasion of several *Salmonella* serovars into host epithelial cells. In addition, we show that the closely related human tetraspanin CD9 co-localizes with human CD81 during *Salmonella* invasion but does not contribute to invasion.

Materials and Methods

Tissue culture preparation

HepG2 (ATCC HB-8065) and HT29-MTX-E12 [19] (a kind gift from Marguerite Clyne, University College Dublin) cells were grown in Dulbecco's modified Eagle's medium with 10% fetal calf serum (FCS) (Merck) and 1x non-essential amino acids (Gibco). Caco2 clone C2BBe1 cells (ATCC, CRL-2102™) were maintained in the same medium with the addition of 10 µg/ml holotransferrin (Sigma).

Bacterial culture preparation

Salmonella strains listed in Table S1, were grown in lysogeny broth (LB) and harvested at an early log growth phase. *Listeria monocytogenes* was grown in Brain Heart Infusion.

Tetraspanin overexpression in HepG2 cells

HepG2 cells (which do not express CD81 [12]) were transduced to overexpress human CD81, human CD9 or rat CD81 using a lentiviral packaging system as previously described [20]. Briefly,

lentiviral pseudoparticles encoding either human CD81, rat CD81 or human CD9 were generated using a three-plasmid system (Table S2): a plasmid encoding vesicular stomatitis virus G (VSV-G) protein, a plasmid encoding HIV gag-pol as well as pTRIP-hCD81, pTRIP-CD9 or pTrip-rCD81 mixed in 1:3:3 ratios. HepG2 cells were seeded at 8.0×10^4 cells per well of a six-well plate and infected 24 h later with the packaged lentivirus in DMEM supplemented with 3% FCS and 4 µg/ml polybrene (Sigma) for 6 hours followed by replenishment with fresh culture medium. Transduced cells were manually sorted by flow cytometry using Becton-Dickinson FACSAria III Fusion by the Hannover Medical School FACS core facility. Flow cytometry analyses were done by using FlowJo v.10 software. Table S3 lists the antibodies used for flow cytometry.

Generation of CD81- and CD9-deficient intestinal cell lines by CRISPR/Cas9

CD81 synthetic guide RNA (5'-TGGTGGTCTGCGGGTCATGG-3'), CD9 synthetic guide RNA (5'- GCGACATACCGCATAGTGGA -3') or a scrambled sequence as control guide RNA (5'-CTAAGGTTAAGTCGCCCTCG-3') cloned into pLentiCRISPR V2 (a gift from Feng Zhang (Addgene plasmid #52961; http://n2t.net/addgene:52961; RRID:Addgene_52961) was incorporated into a lentiviral packaging system (Table S2) [12]. C2BBe1 and HT29-MTX-E12 cells seeded at 3 $x10^5$ in 6-well plates were transduced with the lentiviral particles encoding either the CD81 guide RNA, CD9 guide RNA or scrambled sequence. Cells were selected with puromycin and stained with anti-human CD81-APC or isotype-matched IgG1 kappa. Cells were gated for single cells not expressing CD81 or CD9, respectively, and were sorted by flow cytometry using Becton-Dickinson FACSAria III. CD81(-) or CD9(-)cells were seeded into fresh culture medium, expanded and maintained in medium containing 1 µg/ml puromycin.

Adhesion assay

C2BBe1 cells were seeded at 1.0 x 10^5 cells in 24-well tissue culture plates (Sarstedt) 48 hours prior to infection. Prior to infection, medium was replaced by cold (4ºC) medium and cells were infected at an MOI of 100 at 4ºC for 60 minutes. Cells were washed 3x with 1 ml of PBS per well before cells were lysed with lysis buffer (PBS containing 1% (v/v) Triton X-100, 0.1% (v/v) sodium dodecyl sulfate (SDS)). Cell lysates were serially diluted in PBS and plated on LB agar plates. The

percentage of adhesion was calculated as the ratio of the CFU/well recovered from the cell lysates to the CFU/well of the inoculum.

Gentamicin killing assay

HepG2 and HT29-MTX-E12 cells were seeded in 24-well plates at a density of $2x10^5$ cells/well one day prior to infection. C2BBe1 cells were seeded at 1.0 x 10^5 cells in 24-well tissue culture plates (Sarstedt), 48 hours prior to infection. Cells were cultured in their respective media and incubated in 5% CO_2 at 37°C. One hour prior to infection, medium was exchanged to serum-free culture medium. Cells were infected at an MOI 10 for 30 min (*S.* Tm SL1344, *S.* Enteritidis LA5, *S.* Infantis 119944, *S.* Paratyphi A 45157) or 60 minutes (*S.* Tm 14028s, 14028s/3Δ or 14028s/3 Δ+rck) at 37ºC with 5% CO_2; non-adherent bacteria were removed by washing with phosphate-buffered saline solution (PBS) with Mg^{2+} and Ca^{2+} (Gibco). To enumerate host-associated bacteria (which includes early invaded and cell-adherent bacteria), cells were lysed with lysis buffer. Cell lysates were collected, and serial dilutions plated on LB agar plates. The percentage of host association was calculated as CFU/well recovered from cell lysates normalized to the CFU/well of inoculum.

To quantify bacterial invasion, unbound extracellular bacteria were removed by three washes with PBS and culture medium containing 100 µg/ml gentamicin was added. Cells were further incubated for one hour to kill remaining extracellular bacteria. After three washes with PBS internalized bacteria were recovered by lysing host cells and plating serial dilutions as described above. Bacterial colonies were counted and invasion was calculated as the ratio of the CFU/well recovered from the cell lysates to the CFU/well of inoculum.

CD81 Antibody blocking

Cells were treated with mouse anti-human CD81 (clone JS-81 RUO, RRID no. AB_396028) or its mouse IgG1 isotype-matched control (clone MOPC-21, RRID no. AB_396088) (Table S4) for 1 hour at 37°C prior to infection. 30 min post infection, cells were washed 3x with 1 ml of PBS per well before cells were lysed with lysis buffer. The amount of host-associated *Salmonella* was enumerated by plating serial dilutions of the cell lysates.

HCV E2 blocking

Recombinant HCV E2 was produced as described previously [21]. HepG2 cells were incubated with soluble HCV E2 at indicated concentrations in serum free media for one hour followed by infection with *S*. Tm SL1344 at an MOI 10 for 30 minutes. Then, 100 µg/ml gentamicin was added, and the amount of intracellular *Salmonella* was enumerated 1.5 h post infection.

Cell surface cholesterol depletion

Cell surface cholesterol depletion was carried out according to established methods [22]. Briefly, cell monolayers were incubated with 10 mM methyl-□-cyclodextrin (M□CD, Sigma) in serum free medium at 37°C for 15 minutes followed by infection with *S*.Tm. Infection and gentamicin killing assay were performed as described above.

Immunofluorescence microscopy

C2BBe1 cells were seeded on glass coverslips in 24 well plates. After infection with GFP-expressing *S*.Tm SL1344 (MOI 100, 15 min), samples were fixed using 4% PFA, washed three times with PBS and blocked and permeabilized with a buffer solution containing 10% normal goat serum, 0.1% Triton X-100, 0.05% Tween 20 in PBS. Primary and secondary antibodies (Table S5) were diluted in the same buffer. Host cell nuclei were detected using 4′,6-diamidino-2-phenylindole, dilactate (DAPI, Invitrogen). F-actin was detected using Phalloidin-iFluor647 (Abcam) and cells were mounted using Dako mounting medium.

Proximity Ligation Assay

Proximity ligation assays were performed using the Red Duolink *in situ* PLA Kit (Sigma-Aldrich). Briefly, C2BBe1 cells were seeded in an 8-well chamber slide at $5x10^4$ cells per well and were infected with *S*. Tm SL1344/pFPV25.1 at an MOI 100. 15 minutes post-infection, cells were washed 3x with PBS followed by PFA-fixation and permeabilization and blocking with PBS containing 10% normal goat serum, 0.1% Triton X-100, 0.05% Tween 20. Cells were immunolabeled with rabbit anti-human CD81 (RRID: AB_2789447) and mouse anti-human CD9 (RRID: AB_314907). PLA was performed using secondary antibodies, ligase, amplification and detection reagents included in the kit according to the manufacturer's protocol.

Image Acquisition and Analysis

Microscopy and Image acquisition was done using a Zeiss Apotome 2 (Fig. 2E and Fig. 4C, Fig. 5C, Fig. S4, Fig. S5) or a Leica Thunder Live Cell imaging platform (Fig. 3, Fig. S2) for widefield imaging or with a Zeiss LSM 980 with Airyscan 2 (Fig. 5A) for laser confocal imaging performed at the Research Core Unit for Laser Microscopy, Hannover Medical School. Image data were visualized and analysed using Zen Blue 3.4, Leica LAS X software and FIJI/ImageJ software. To quantify CD81 in *S.*Tm-induced ruffles, images were taken on a Zeiss Apotome 2 with at a magnification of 200X at eight random fields of view (FOV). Cells with invasion events with ruffles were counted and normalized by the total number of infected cells. CD81 staining was assessed in ruffles.

Multiple sequence alignment

For the multiple sequence alignment (MSA), sequence data were acquired from the publicly available protein database UniProt. Specifically, sequences for the proteins CD81_HUMAN (UniProt: P60033), CD81_MOUSE (UniProt: P35762) and CD81_RAT (UniProt: Q62745) were selected. The MSA was conducted using the Clustal Omega (ClustalO) server (https://www.ebi.ac.uk/Tools/msa/clustalo/). The alignment was carried out using the default parameters with the output format set to "ClustalW". To visualize the MSA, the CLC Sequence Viewer 8.0 (qiagenbioinformatics.com) was utilized.

Statistical Analysis

Data were analyzed using GraphPad Prism V8.4.3 software (Graphpad Software, LLC). Graphs display the mean values ± SD of a representative experiment out of three independent experiments unless otherwise stated. One-way analysis of variance (ANOVA) with post-hoc Tukey's multiple comparison test, or unpaired two-tailed Student's t-test, were used in the statistical analysis, as indicated. P-values smaller than 0.05 were considered statistically significant.

Results

Tetraspanin CD81 overexpression in epithelial cells contributes to the invasion of various *Salmonella* strains

Here, we were interested in clarifying the role of CD81 during *Salmonella* infection of epithelial cells. We created a HepG2 cell line with CD81 cell surface overexpression by lentiviral transduction. The resulting cells were validated by flow cytometry for surface expression of CD81 (Figure 1A). As previously reported [12], CD81 surface expression is absent on wild-type HepG2 cells (gray histogram) whereas HepG2 cells overexpressing hCD81 show high CD81 surface expression (red histogram). The sorted cells were expanded and used for infection experiments with *S.* Typhimurium (*S.* Tm) SL1344. Host-associated (30 min post infection which include adherent and early invaded bacteria) and intracellular bacteria (1.5 h post infection) were recovered and enumerated as described in Materials and Methods. As shown in Figure 1B and 1C, *S.* Tm SL1344 associated and invaded significantly better into HepG2 cells overexpressing human CD81 compared to wild-type HepG2 cells. *Salmonella* serovars differ in their efficiency to invade into epithelial cells. Therefore, to test if the effect of CD81 is strain-dependent, different representative non-typhoidal and typhoidal *Salmonella* strains were tested. In addition to *S.* Typhimurium, *S.* Enteritidis, and *S.* Infantis were used to represent the most epidemiologically prevalent non-typhoidal *Salmonella* serovars reported in the EU [1] and the typhoidal serovar *S.* Paratyphi A as an emergent strain causing major disease burden particularly in Asia [23] (Figure 1BC). In all cases, the overexpression of human CD81 was observed to enhance *Salmonella* invasion in HepG2 cells compared to the absence of CD81 (wild-type HepG2). This indicates that CD81 facilitates adhesion and invasion of various *Salmonella* serovars into HepG2 epithelial cells.

S. Tm primarily invades host cells through a trigger-like invasion mechanism mediated by a Type III secretion system (T3SS-1) encoded by the *Salmonella* Pathogenicity Island-1 (SPI-1) followed by macropinocytosis of the bacteria into the host cell [24]. However, *S.* Tm can also invade host cells via a zipper-like invasion mechanism mediated by the outer membrane proteins Rck or PagN [18,25]. Furthermore, an *S.* Tm mutant strain lacking the three known invasins InvA (without T3SS-1), PagN and Rck ("3Δ" mutant) was demonstrated to invade multiple epithelial host cell lines

in a primarily zipper-like invasion process [26]. We tested whether CD81 could support T3SS-1-independent bacterial internalization. *S*. Tm 3Δ and its *rck*-complemented counterpart associated with HepG2 cells significantly more when CD81 is present on the host cell surface (Figure 1D). However, the proportion of intracellular *S*. Tm 3Δ and *S*. Tm 3Δ + *rck* bacteria recovered after invasion was very low and not significantly dependent on CD81 in contrast to the parental wild-type strain *S*.Tm 14028s (Figure 1E).

Previous studies have identified an HCV E2 binding domain in the LEL region of human CD81 which is important for HCV entry into hepatocytes [27]. To test whether the LEL mediates invasion of *S*. Tm into epithelial cells, increasing concentrations of HCV E2 glycoprotein were added to HepG2 cells (with and without CD81-overexpression) one hour prior to infection with *S*. Tm. Increasing concentrations of HCV E2 resulted in a dose-dependent reduction of *Salmonella* invasion into CD81-overexpressing HepG2 cells (Figure 1F, *red bars*) but HCV E2 treatment did not affect *Salmonella* internalization into CD81-deficient wildtype HepG2 cells (*black bars*). We performed a similar experiment on intestinal epithelial HT29-MTX-E12 cells using an anti-CD81 mAb that specifically binds to the CD81-LEL domain [27] and noted a significant reduction of *S*. Tm associated with host cells upon antibody treatment (Figure S1A). These data demonstrate that blocking the LEL domain exerts an inhibitory effect towards CD81-dependent *Salmonella* association with intestinal epithelial cells.

Deletion of CD81 in intestinal epithelial cells attenuates *S*. Typhimurium internalization.

We further investigated the role of CD81 in two commonly used intestinal epithelial cell lines, HT29-MTX-E12 and C2BBe1 [28]. We used CRISPR/Cas9 to create CD81-deficient intestinal epithelial cell lines as described in Materials and Methods. Figure 2A and S1B, show the flow cytometry analysis of CD81 (+) and CD81-KO cell populations of C2BBe1 and HT29-MTX-E12, respectively. These cells were then infected with *S*. Tm and adhesion and invasion were analyzed. Our results show that deletion of CD81 in both cell lines resulted in fewer host cell associated *Salmonella* (host cell association includes early invaded and adherent *Salmonella*) and in less efficient invasion of

Salmonella into the cells compared to WT cells (Figure 2BC and S1C). As a control, we quantified invasion of *Listeria monocytogenes* (Figure 2D) which was previously shown that its invasion into HeLa cells is partially dependent on CD81 [13]. To distinguish between a role of CD81 in adhesion and in invasion we followed two approaches: first, C2BBe1 cells were infected with GFP-expressing *S.* Tm at 4°C to inhibit *Salmonella*-induced actin polymerization and subsequent bacterial uptake while allowing *Salmonella* to bind to the host cell surface. Imaging data revealed cytoplasmic, perinuclear and faint membrane staining of CD81 but no major CD81 recruitment to *Salmonella* adhesion sites (Figure 2E). Non-infected control cells grown at 37°C show a similar distribution of CD81 (Figure S2). These observations are confirmed by the results of the bacterial adhesion assay performed at 4°C (Figure 2F) where no differences were found in number of bacteria adhering to CD81(+) compared to CD81-KO cells, indicating that CD81 does not influence *Salmonella* adhesion to C2BBe1 cells. However, at 4°C not only invasion of *Salmonella* but also CD81 trafficking is most likely abrogated. Therefore, we used the *S.* Tm 3Δ and *S.* Tm 3Δ+rck mutants that adhere well to epithelial cells but do not efficiently invade. We observed that there is no significant difference for adhesion or invasion of *S.* Tm 3Δ mutant into CD81 wt or CD81-deficient C2BBe1 cells (Fig. 2BC). Taken together, these data suggest that uptake of *Salmonella* into C2BBe1 epithelial cells, but not adhesion to the epithelium, drives CD81 localization to the *Salmonella* entry site.

Cell surface cholesterol depletion impacts CD81-dependent *Salmonella* invasion

Previous studies have found that membrane cholesterol plays a role in the invasion of different pathogens such as *Listeria monocytogenes* [29], *Salmonella* [30], and *Plasmodium* [22]. CD81 is known to possess a cholesterol-binding pocket in its central cavity [5] which dictates its structural conformation and affects interactions with other ligands [31] that may associate within the tetraspanin-enriched microdomain (TEM). To test whether CD81-mediated enhancement of *Salmonella* invasion into host cells is cholesterol-dependent, we depleted cholesterol using methyl-β-cyclodextrin (MβCD), which sequesters cholesterol in cell membranes. To this end, wildtype and CD81-KO C2BBe1 cells were pre-treated with MβCD prior to *S.* Tm SL1344 infection. Our data show that MβCD-treatment of CD81(+) C2BBe1 cells results in a significant reduction of *Salmonella* invasion, whereas cholesterol

depletion did not significantly affect *S*. Tm invasion into CD81-deficient cells (Figure 2G) indicating that the CD81-mediated *Salmonella* internalization into host cells may be cholesterol-dependent.

CD81 localizes to actin-enriched membrane ruffling regions triggered by *Salmonella* invasion

To visualize CD81 during *Salmonella* invasion, C2BBe1 cells were infected with GFP-expressing *S*. Tm and CD81 and F-actin were analyzed using immunofluorescence staining. Membrane ruffles during early *Salmonella* invasion are indicated by the localized presence of massive cytoskeletal rearrangements around *Salmonella* entry sites (Figure 3A). In addition to the cytoplasmic staining pattern, recruitment of CD81 to areas also enriched in F-actin around invading *Salmonella* is apparent (Figure 3A, *region of interest*). This data shows that CD81 locally reorganizes around the invasion foci on the host cell surface during invasion into C2BBe1 cells. Quantification of GFP-expressing *S.*Tm invasion triggering ruffle formation showed that approximately 10% of invasion events were associated with ruffles. Ruffles were almost exclusively CD81-positive (Figure 3B).

Human CD81 but not rat CD81 drives *Salmonella* invasion

For certain viruses (e.g. HCV), uptake is mediated exclusively by human CD81, while for other viruses (e.g. Chikungunya virus) both human and rodent CD81 can mediate virus replication [32]. The amino acid sequences of human and rat CD81 share 93% identity (Table S6) based on sequence alignment with Clustal Omega and highest sequence variability lies within the LEL region (Figure S3). Previous studies have speculated that sequence variation within and outside the LEL region might have implications for structure-function attribution of tetraspanins [11]. To test whether host species-specific CD81 is important for *S*. Tm invasion, we compared human CD81 and rat CD81 overexpressed in HepG2 cells (Figure 4A). Invasion assays demonstrate that overexpression of rat CD81 in HepG2 cells did not promote *S*. Tm invasion compared to human CD81, indicating a species-specific effect of human CD81 (Figure 4B).

Role of CD9 in *S*. Typhimurium uptake into epithelial cells

CD9, another tetraspanin that has been reported to interact with CD81 [33] was also tested to see if it can enhance *S*. Tm uptake. We noted a basal CD9 gene expression in HepG2 cells and that CD81 overexpression slightly upregulates CD9 expression as well (data not shown). We investigated the localization of CD9 during early *Salmonella* invasion at 15 minutes post-infection.

Immunostaining of CD9 in GFP-expressing *S*.Tm-infected C2BBe1 cells revealed that CD9 localizes to *Salmonella* entry sites along with F-actin (Figure 4C). Analysis of the role of CD9 in *Salmonella* adhesion and invasion in HepG2 cells overexpressing CD9 revealed that, CD9 facilitates *Salmonella* invasion but does not influence *Salmonella* adhesion (Figure 4DE). Staining of CD9 in HepG2 wt cells was weak, while a clear pattern was seen in HepG2/hCD9 cells (Figure S4A). The distribution of CD9 was comparable to the distribution in C2BBe1 cells with partial localization of CD9 with actin and partial co-localization with invading *S*.Tm (Figure S4A, yellow arrowheads). Of note, overexpression of hCD9 in HepG2 cells did not affect CD81 expression (Figure S4B). Next, we generated C2BBe1 lacking CD9 using CRISPR/Cas9 as described in Materials and Methods. In contrast to the results obtained in HepG2 cells, however, infection of C2BBe1 wt and *CD9*$^{-/-}$ cells showed no role for CD9 in adhesion or invasion of *S.* Typhimurium (Fig 4FG). Altogether, these observations suggest that although CD9 is recruited to the *Salmonella* invasion site, it is not required for *Salmonella* adhesion or invasion into C2BBe1 cells.

CD9 and CD81 are both recruited to the *Salmonella* entry site during the early phase of cellular invasion

Previous reports have noted that CD9 and CD81 are frequently found together in tetraspanin-enriched microdomains [33]. Thus, we investigated if CD9 and CD81 interact with each other and assessed the spatial localization of CD9 and CD81 during *Salmonella* invasion. Double immunostaining for CD81 and CD9 in C2BBe1 cells after GFP-expressing *S*.Tm infection revealed that both tetraspanins partially co-localize at the *Salmonella* entry site (Figure 5A).

To further clarify whether CD9 and CD81 were indeed recruited together as partner proteins during *Salmonella* invasion, we performed an *in situ* proximity ligation assay (PLA) after immunolabelling CD9 and CD81 in C2BBe1 cells infected with *S*.Tm. PLA detects proteins that are at most 40 nm apart, indicating not only proximity but also likely protein-protein interaction [34] as illustrated in a schematic diagram in Figure 5B. PLA signals (red) probing CD9/CD81 interaction were observed to be clustered near the entry point of *Salmonella* during invasion but also in the cytoplasm (Figure 5C). The PLA signal was found to be specific for detecting a complex of CD9 and CD81. The control set up omitting either anti-CD81, anti-CD9 or all primary antibodies gave no

fluorescence signal which further validates that PLA signals were specific for the close interaction of CD9 and CD81 (Figure S5). This data confirms the previous observation from double immunostaining using anti-CD81 and anti-CD9 antibodies where we observed that both CD9 and CD81 co-localize at the *Salmonella* invasion foci (Figure 5A), indicating a protein complex formation of these tetraspanins during *S.* Tm invasion.

Discussion

It is well documented that many pathogens hijack tetraspanins to their own advantage to facilitate colonization of host cells [8,9]. In recent years, several studies have shown that tetraspanins contribute to the entry and invasion process of various pathogens including viruses, bacteria, and parasites. Our results show that overexpression of human CD81 in HepG2 cells leads to an enhancement of *Salmonella* invasion compared to wild-type HepG2 cells. Furthermore, we observed this effect for typhoidal and non-typhoidal *Salmonella* strains, indicating an active involvement of CD81 during *Salmonella* invasion in clinically and epidemiologically relevant strains.

We demonstrate a species-specific role of human CD81 for the invasion of *Salmonella* into human epithelial cells. Overexpression of rat CD81 in HepG2 cells did not increase the efficiency of *S.* Typhimurium invasion compared to an overexpression of human CD81. We assume that there is species-specificity for tetraspanins to cluster together based on their sequence alignment and homology (Figure S3, Table S6) as the sequence affects protein folding and exposed interaction residues for partner proteins. For example, overexpression of rat CD81 in HepG2 cells does not enhance HCV infectivity [35]. This may be because human CD81 bears a unique binding site for the HCV E2 ectodomain at the human CD81-LEL, based on previous studies which demonstrated that the LEL α-helices are also important for homomeric clustering among CD81 molecules and heteromeric clustering with their partner proteins *i.e.* CD9 or CD151 [6].

Infection of epithelial cells, the primary target for *Salmonella* infection, demonstrated that loss of CD81 expression reduced *Salmonella* invasion, further validating the importance of CD81 on the host cell surface during *Salmonella* invasion. Earlier studies have found that downregulating CD81 expression in HeLa cells using siRNA reduces *Listeria monocytogenes* invasion which invades in a

zipper-like manner [13]. Furthermore, previous studies have also demonstrated that siRNA knockdown of CD81 in primary human hepatocytes reduces the amount of internalized *P. falciparum* exo-erythrocytic forms recovered from infected hepatocytes [22]. On the other hand, other investigators found that a CD81 knockout in A549 cells has no effect on invasion of *Burkholderia pseudomallei* [15].

Previous studies have demonstrated the importance of cholesterol in *Salmonella* invasion [30]. Furthermore, other studies have shown that cholesterol depletion also reduced *Listeria monocytogenes* invasion [29] and that cholesterol-rich cells at the metaphase stage are preferential targets for *Salmonella* invasion [30]. In our study, we found that cholesterol depletion prior to *Salmonella* infection of C2BBe1 cells has a more pronounced effect on bacterial invasion in the presence of CD81. This might be due to the fact that CD81 possesses a cholesterol-binding pocket which affects its conformational structure and subsequent interaction with host proteins [5]. Another explanation could be the fact that CD81 can sequester cholesterol and that CD81-cholesterol interactions affect TEM organization and membrane deformations thereby influence bacterial uptake [36].

Using microscopy and image analysis, we observed that CD81 recruitment and redistribution occurs at the invasion foci of *Salmonella* (marked by actin polymerization and membrane ruffle formation) as early as 15 minutes of infection. Inhibiting *Salmonella* uptake by incubating cells at 4°C during infection also inhibited trafficking and recruitment of CD81 into the *Salmonella* adhesion site. As *Salmonella* adhesion is not affected during these conditions, these observations suggest that CD81 does not play a role in *Salmonella* adhesion but only during an active invasion event. Since *Salmonella* strains used for infection experiments were cultivated under SPI-1 inducing conditions, coupled with observations of massive membrane ruffles (which were predominantly CD81-positive) and actin polymerization around the *Salmonella* invasion foci, it could be concluded that CD81 participates in a trigger-like entry of *Salmonella* into host cells. Additionally, we tested a triple mutant *S.* Tm 14028s/3Δ, (*invA, pagN* and *rck*) which had been found to have severely reduced invasion efficiency in various cell lines [26]. We observed that *rck*-complemented *S.* Tm 14028s/3Δ rck mutant showed enhanced CD81 dependent host cell association but not increased CD81-dependent invasion in HepG2 cells. However, it must be noted that invasion of *S.* Tm 14028s/3Δ and *rck*-complemented *S.* Tm

14028s/3Δ strains in HepG2 cells was very low, limiting the informative value of this invasion experiment. It has been reported that zipper-like invasion by *Salmonella* can be induced by growing the bacteria in the presence of acyl homoserine lactones and inducing a swarming behavior and expression of SdiA - a LuxR homolog which detects AHLs from other bacteria and upregulate the rck operon [37]. Furthermore, other investigators have found that *S.* Tm exhibits a discrete invasion mechanism in the murine gut driven by the T3SS-1 effector, SipA [38]. However, our data implicate that CD81 rather supports trigger-like invasion of *Salmonella* into host cells.

Antagonizing the effect of CD81 on *Salmonella* invasion by targeting it at the LEL with CD81-mAbs or HCV E2-derived glycoproteins demonstrated that the LEL region specifically influences *Salmonella* invasion. CD81 has been demonstrated as a direct receptor for HCV E2 glycoprotein, specifically interacting with the LEL domain of CD81 [39,40] and that saturating the CD81-LEL with HCV E2 reduced the infectivity of HCV particles [21]. These observations support the concept that the LEL region is a critical domain for CD81-dependent entry of *Salmonella*. Interestingly, it has been shown that in anti-CD81 antibodies can block binding of *S.* Tm to macrophages. However, uptake of *Salmonella* by macrophages seems to be CD81-independent but dependent on other tetraspanins [16]. This points to a cell-type specific role of CD81 for *S.* Tm infection.

Similar to CD81, CD9 also localizes to the *Salmonella* entry site. Although CD9 seemed to facilitate *Salmonella* invasion when overexpressed in HepG2 cells, we did not see decreased uptake in *CD9*-deficient C2BBe1 cells. In addition, CD9 did not promote *Salmonella* adhesion. Therefore, we conclude that CD9 itself is not necessary for *Salmonella* invasion at least into C2BBe1 intestinal epithelial cells. Double immunostaining of CD81 and CD9 further revealed that both tetraspanins are recruited to the entry site of *Salmonella* and the PLA assay demonstrated that CD81 and CD9 co-localize to tetraspanin webs at the *Salmonella* entry site. CD9 is a tetraspanin often reported to be an interactor with CD81 and these tetraspanins co-localize also in absence of infection [33,41]. Other studies demonstrate that CD63 and CD151 also associate within this tetraspanin network. Furthermore, high-resolution imaging of primary endothelial cells demonstrated that CD9 recruits ICAM-1 clusters following stimulation with TNF-α [42]. The authors noted that CD9 clusters around

cellular protrusions primarily in microvilli and lamellipodia and that a knockdown of CD9 dysregulates its association with adhesion factors such as JAM-A and ICAM-1, and consequently reduces cellular protrusions and microvilli formation [42]. It could be hypothesized that CD9 clustering (together with CD81 and other partner proteins) coordinates cellular microvilli formation followed by an increasing recruitment of CD81 as membrane ruffle formation becomes more pronounced. Two previous studies independently observed that CD81 is coupled to Rac, independent of its activation and this direct interaction is essential for the formation of membrane protrusions and cell migration [43]. Thus, CD9 and CD81 could potentially play a role in membrane curvature and protrusion processes considering their high degree of localization in such cellular structures.

Furthermore, CD9 and CD81 have been shown to play a role in membrane fusion [15]. These tetraspanins may play a role in the macropinocytosis by facilitating membrane ruffling and remodelling to allow efficient enclosure of the bacteria into a host-derived vacuolar membrane called the *Salmonella*-containing vacuole during the macropinocytotic process. Indeed, tetraspanins can modify the biophysical characteristics of the cell membrane, to control the morphogenesis of membrane protrusive structures such as the membrane curvature or the membrane connections of the cytoskeletal network [31,43]. Moreover, the tetraspanin CD82 is recruited to phagosomes containing internalized bacterial pathogens (*Escherichia coli* and *Staphylococcus aureus*) and fungal pathogens (*Cryptococcus neoformans*, *Candida albicans* and *Aspergillus fumigatus*) [44]. As tetraspanins are known to exhibit functional redundancy and interact with each other, the independent overexpression of either CD9 or CD81 in HepG2 may promote membrane curvature and invasion of *Salmonella* by properly localizing receptors and host proteins at the invasion foci. This process then supports the internalization and enclosure of the bacteria into an SCV.

In summary, we demonstrate that CD81 is recruited to the site of the invasion foci, following the action of secreted effectors or binding of an unknown bacterial ligand to a host receptor and other host proteins in a tetraspanin-enriched microdomain. This cascade of events causes membrane ruffling on the host cell surface and localized formation of F-actin polymers at the invasion foci, perhaps through a Rac-dependent mechanism. Macropinocytotic uptake and internalization of the bacteria is then facilitated by tetraspanins, leading to the engulfment of *Salmonella* into the SCV.

Author contributions

Kris Alvarez, Lisa Lasswitz, Francisco J. Zapatero-Belinchón, Kumar Nagarathinam, Thomas Krey, Agnes Wiedemann, Gisa Gerold, Guntram Grassl: conception and design; Kris Gerard Alvarez, Lisa Goral, Abdulhadi Suwandi, Katrin Ehrhardt, Katrin Künnemann, Guntram Grassl: data acquisition and analysis; Kris Alvarez, Guntram Grassl drafted the initial version of the manuscript; all authors: critical revision of the manuscript for intellectual content; all authors approved the final version of the manuscript; all authors agree to be accountable for all aspects of the work.

Acknowledgements

We would like to thank Charlie Rice and Thomas von Hahn for the pTRIP-hCD81, pTRIP-CD9 and pTrip-rCD81 constructs and Marc Schmidt-Supprian, Klaus Heger for the pLenti CRISPR v2 ccdB plasmid and Philippe Velge for the *S*. Tm 3Δ mutant strain. We would also like to acknowledge Daniel Marke for his contributions on the sequence alignment and visualization of tetraspanin peptide sequences. We are also grateful for the technical assistance of the Cell Sorting Core Facility (supported in part by the Deutsche Forschungsgemeinschaft) and the Research Core Unit for Laser Microscopy at the Hannover Medical School.

Funding Information

This work was supported by the Deutsche Forschungsgemeinschaft (DFG) collaborative research center SFB 900 (Project number 158989968) to GAG, TK and GG. KGA was supported by the German Academic Exchange Service DAAD, the Hannover Biomedical Research School (HBRS) and by the Center for Infection Biology (ZIB). This work was also funded by the Ministry of Science and Culture of Lower Saxony and the German Federal Ministry of Education and Research through the Professorinnenprogramm III and the Knut and Alice Wallenberg Foundation to GG.

Disclosure statement

The authors declare no competing interest.

Data availability statement

All data generated during this study are available on figshare. doi.org/10.6084/m9.figshare.26181086.v1 [45].

References

[1] The European Union One Health 2020 Zoonoses Report. EFSA Journal 2021;19. https://doi.org/10.2903/j.efsa.2021.6971.

[2] Hemler ME. Tetraspanin functions and associated microdomains. Nat Rev Mol Cell Biol 2005;6:801–11. https://doi.org/10.1038/nrm1736.

[3] Charrin S, le Naour F, Silvie O, Milhiet P-E, Boucheix C, Rubinstein E. Lateral organization of membrane proteins: tetraspanins spin their web. Biochemical Journal 2009;420:133–54. https://doi.org/10.1042/BJ20082422.

[4] Yáñez-Mó M, Barreiro O, Gordon-Alonso M, Sala-Valdés M, Sánchez-Madrid F. Tetraspanin-enriched microdomains: a functional unit in cell plasma membranes. Trends Cell Biol 2009;19:434–46. https://doi.org/10.1016/j.tcb.2009.06.004.

[5] Zimmerman B, Kelly B, McMillan BJ, Seegar TCM, Dror RO, Kruse AC, et al. Crystal Structure of a Full-Length Human Tetraspanin Reveals a Cholesterol-Binding Pocket. Cell 2016;167:1041-1051.e11. https://doi.org/10.1016/j.cell.2016.09.056.

[6] Schmidt TH, Homsi Y, Lang T. Oligomerization of the Tetraspanin CD81 via the Flexibility of Its δ-Loop. Biophys J 2016;110:2463–74. https://doi.org/10.1016/j.bpj.2016.05.003.

[7] Shoham T, Rajapaksa R, Kuo C-C, Haimovich J, Levy S. Building of the Tetraspanin Web: Distinct Structural Domains of CD81 Function in Different Cellular Compartments. Mol Cell Biol 2006;26:1373–85. https://doi.org/10.1128/MCB.26.4.1373-1385.2006.

[8] van Spriel AB, Figdor CG. The role of tetraspanins in the pathogenesis of infectious diseases. Microbes Infect 2010;12:106–12. https://doi.org/10.1016/J.MICINF.2009.11.001.

[9] Karam J, Méresse S, Kremer L, Daher W. The roles of tetraspanins in bacterial infections. Cell Microbiol 2020;22. https://doi.org/10.1111/cmi.13260.

[10] Cocquerel L, Silvie O. The Role of CD81 in HCV and Plasmodium Infection. Tetraspanins, Dordrecht: Springer Netherlands; 2013, p. 345–86. https://doi.org/10.1007/978-94-007-6070-7_14.

[11] Banse P, Moeller R, Bruening J, Lasswitz L, Kahl S, Khan A, et al. CD81 Receptor Regions outside the Large Extracellular Loop Determine Hepatitis C Virus Entry into Hepatoma Cells. Viruses 2018;10:207. https://doi.org/10.3390/v10040207.

[12] Bruening J, Lasswitz L, Banse P, Kahl S, Marinach C, Vondran FW, et al. Hepatitis C virus enters liver cells using the CD81 receptor complex proteins calpain-5 and CBLB. vol. 14. 2018. https://doi.org/10.1371/journal.ppat.1007111.

[13] Tham TN, Gouin E, Rubinstein E, Boucheix C, Cossart P, Pizarro-Cerda J. Tetraspanin CD81 is required for Listeria monocytogenes invasion. Infect Immun 2010;78:204–9. https://doi.org/10.1128/IAI.00661-09.

[14] Martínez del Hoyo G, Ramírez-Huesca M, Levy S, Boucheix C, Rubinstein E, Minguito de la Escalera M, et al. CD81 Controls Immunity to *Listeria* Infection through Rac-Dependent Inhibition of Proinflammatory Mediator Release and Activation of Cytotoxic T Cells. The Journal of Immunology 2015;194:6090–101. https://doi.org/10.4049/jimmunol.1402957.

[15] Sangsri T, Saiprom N, Tubsuwan A, Monk P, Partridge LJ, Chantratita N. Tetraspanins are involved in Burkholderia pseudomallei-induced cell-to-cell fusion of phagocytic and non-phagocytic cells. Sci Rep 2020;10. https://doi.org/10.1038/s41598-020-74737-y.

[16] Hassuna NA, Monk PN, Ali F, Read RC, Partridge LJ. A role for the tetraspanin proteins in Salmonella infection of human macrophages. Journal of Infection 2017. https://doi.org/10.1016/j.jinf.2017.06.003.

[17] Ménard S, Lacroix-Lamandé S, Ehrhardt K, Yan J, Grassl GA, Wiedemann A. Cross-Talk Between the Intestinal Epithelium and Salmonella Typhimurium. Front Microbiol 2022;13. https://doi.org/10.3389/fmicb.2022.906238.

[18] Barilleau E, Védrine M, Koczerka M, Burlaud-Gaillard J, Kempf F, Grépinet O, et al. Investigation of the invasion mechanism mediated by the outer membrane protein PagN of Salmonella Typhimurium n.d. https://doi.org/10.1186/s12866-021-02187-1.

[19] Dolan B, Naughton J, Tegtmeyer N, May FEB, Clyne M. The Interaction of Helicobacter pylori with the Adherent Mucus Gel Layer Secreted by Polarized HT29-MTX-E12 Cells. PLoS One 2012;7. https://doi.org/10.1371/journal.pone.0047300.

[20] Dull T, Zufferey R, Kelly M, Mandel RJ, Nguyen M, Trono D, et al. A third-generation lentivirus vector with a conditional packaging system. J Virol 1998;72:8463–71. https://doi.org/10.1128/JVI.72.11.8463-8471.1998.

[21] Krey T, D'Alayer J, Kikuti CM, Saulnier A, Damier-Piolle L, Petitpas I, et al. The disulfide bonds in glycoprotein E2 of hepatitis C virus reveal the tertiary organization of the molecule. PLoS Pathog 2010;6. https://doi.org/10.1371/journal.ppat.1000762.

[22] Silvie O, Charrin S, Billard M, Franetich JF, Clark KL, van Gemert GJ, et al. Cholesterol contributes to the organization of tetraspanin-enriched microdomains and to CD81-dependent infection by malaria sporozoites. J Cell Sci 2006;119:1992–2002. https://doi.org/10.1242/jcs.02911.

[23] Sahastrabuddhe S, Carbis R, Wierzba TF, Ochiai RL. Increasing rates of Salmonella Paratyphi A and the current status of its vaccine development. Expert Rev Vaccines 2013;12:1021–31. https://doi.org/10.1586/14760584.2013.825450.

[24] Velge P, Wiedemann A, Rosselin M, Abed N, Boumart Z, Chaussé AM, et al. Multiplicity of Salmonella entry mechanisms, a new paradigm for Salmonella pathogenesis. Microbiologyopen 2012;1:243–58. https://doi.org/10.1002/MBO3.28.

[25] Rosselin M, Virlogeux-Payant I, Roy C, Bottreau E, Sizaret PY, Mijouin L, et al. Rck of Salmonella enterica, subspecies enterica serovar enteritidis, mediates zipper-like internalization. Cell Res 2010;20:647–64. https://doi.org/10.1038/CR.2010.45.

[26] Roche SM, Holbert S, Trotereau J, Schaeffer S, Georgeault S, Virlogeux-Payant I, et al. Salmonella Typhimurium invalidated for the three currently known invasion factors keeps its

ability to invade several cell models. Front Cell Infect Microbiol 2018;8. https://doi.org/10.3389/fcimb.2018.00273.

[27] Harman C, Zhong L, Ma L, Liu P, Deng L, Zhao Z, et al. A View of the E2-CD81 Interface at the Binding Site of a Neutralizing Antibody against Hepatitis C Virus. J Virol 2015;89:492–501. https://doi.org/10.1128/JVI.01661-14.

[28] Gagnon M, Zihler Berner A, Chervet N, Chassard C, Lacroix C. Comparison of the Caco-2, HT-29 and the mucus-secreting HT29-MTX intestinal cell models to investigate Salmonella adhesion and invasion. J Microbiol Methods 2013;94:274–9. https://doi.org/10.1016/j.mimet.2013.06.027.

[29] Seveau S, Bierne H, Giroux S, Prévost M-C, Cossart P. Role of lipid rafts in E-cadherin– and HGF-R/Met–mediated entry of Listeria monocytogenes into host cells. Journal of Cell Biology 2004;166:743–53. https://doi.org/10.1083/jcb.200406078.

[30] Santos AJM, Meinecke M, Fessler MB, Holden DW, Boucrot E. Preferential invasion of mitotic cells by Salmonella reveals that cell surface cholesterol is maximal during metaphase. J Cell Sci 2013;126:2990–6. https://doi.org/10.1242/jcs.115253.

[31] Palor M, Stejskal L, Mandal P, Lenman A, Alberione MP, Kirui J, et al. Cholesterol sensing by CD81 is important for hepatitis C virus entry. Journal of Biological Chemistry 2020;295:16931–48. https://doi.org/10.1074/JBC.RA120.014761/ATTACHMENT/058083F8-CA16-4CCA-AE1C-020BA4677C09/MMC1.ZIP.

[32] Lasswitz L, Zapatero-Belinchón FJ, Moeller R, Hülskötter K, Laurent T, Carlson L-A, et al. The Tetraspanin CD81 Is a Host Factor for Chikungunya Virus Replication. MBio 2022;13. https://doi.org/10.1128/mbio.00731-22.

[33] Frolikova M, Manaskova-Postlerova P, Cerny J, Jankovicova J, Simonik O, Pohlova A, et al. CD9 and CD81 Interactions and Their Structural Modelling in Sperm Prior to Fertilization. Int J Mol Sci 2018;19:1236. https://doi.org/10.3390/ijms19041236.

[34] Bagchi S, Fredriksson R, Wallén-Mackenzie Å. In Situ Proximity Ligation Assay (PLA), 2015, p. 149–59. https://doi.org/10.1007/978-1-4939-2742-5_15.

[35] Flint M, von Hahn T, Zhang J, Farquhar M, Jones CT, Balfe P, et al. Diverse CD81 proteins support hepatitis C virus infection. J Virol 2006;80:11331–42. https://doi.org/10.1128/JVI.00104-06.

[36] Caparotta M, Masone D. Cholesterol plays a decisive role in tetraspanin assemblies during bilayer deformations. Biosystems 2021;209:104505. https://doi.org/10.1016/J.BIOSYSTEMS.2021.104505.

[37] Mijouin L, Rosselin M, Bottreau E, Pizarro-Cerda J, Cossart P, Velge P, et al. Salmonella enteritidis Rck-mediated invasion requires activation of Rac1, which is dependent on the class I PI 3-kinases-Akt signaling pathway . The FASEB Journal 2012;26:1569–81. https://doi.org/10.1096/fj.11-189647.

[38] Fattinger SA, Böck D, di Martino ML, Deuring S, Samperio Ventayol P, Ek V, et al. Salmonella Typhimurium discreet-invasion of the murine gut absorptive epithelium. PLoS Pathog 2020;16:e1008503. https://doi.org/10.1371/journal.ppat.1008503.

[39] Vasiliauskaite I, Owsianka A, England P, Khan AG, Cole S, Bankwitz D, et al. Conformational Flexibility in the Immunoglobulin-Like Domain of the Hepatitis C Virus Glycoprotein E2. MBio 2017;8. https://doi.org/10.1128/MBIO.00382-17.

[40] Koutsoudakis G, Herrmann E, Kallis S, Bartenschlager R, Pietschmann T. The Level of CD81 Cell Surface Expression Is a Key Determinant for Productive Entry of Hepatitis C Virus into Host Cells. J Virol 2007. https://doi.org/10.1128/JVI.01534-06.

[41] Gustafson-Wagner E, Stipp CS. The CD9/CD81 Tetraspanin Complex and Tetraspanin CD151 Regulate α3β1 Integrin-Dependent Tumor Cell Behaviors by Overlapping but Distinct Mechanisms. PLoS One 2013;8:e61834. https://doi.org/10.1371/journal.pone.0061834.

[42] Franz J, Brinkmann BF, König M, Hüve J, Stock C, Ebnet K, et al. Nanoscale Imaging Reveals a Tetraspanin-CD9 Coordinated Elevation of Endothelial ICAM-1 Clusters. PLoS One 2016;11:e0146598. https://doi.org/10.1371/journal.pone.0146598.

[43] Tejera E, Rocha-Perugini V, López-Martín S, Ṕrez-Hernández D, Bachir AI, Horwitz AR, et al. CD81 regulates cell migration through its association with Rac GTPase. Mol Biol Cell 2013;24:261–73. https://doi.org/10.1091/mbc.E12-09-0642.

[44] Artavanis-Tsakonas K, Kasperkovitz P v., Papa E, Cardenas ML, Khan NS, van der Veen AG, et al. The Tetraspanin CD82 Is Specifically Recruited to Fungal and Bacterial Phagosomes prior to Acidification. Infect Immun 2011;79:1098–106. https://doi.org/10.1128/IAI.01135-10.

[45] Grassl G. raw data CD81 manuscript 2024. https://doi.org/10.6084/m9.figshare.26181086.v1.

[46] Hoiseth SK, Stocker BAD. Aromatic-dependent Salmonella typhimurium are non-virulent and effective as live vaccines. Nature 1981;291.

[47] Matsuura M, Kawasaki K, Kawahara K, Mitsuyama M. Evasion of human innate immunity without antagonizing TLR4 by mutant Salmonella enterica serovar Typhimurium having penta-acylated lipid A. Innate Immun 2012;18:764–73. https://doi.org/10.1177/1753425912440599.

[48] Allen-Vercoe E, Dibb-Fuller M, Thorns CJ, Woodward MJ. SEF17 fimbriae are essential for the convoluted colonial morphology of Salmonella enteritidis. FEMS Microbiol Lett 1997;153:33–42. https://doi.org/10.1111/J.1574-6968.1997.TB10460.X.

[49] Aviv G, Tsyba K, Steck N, Salmon-Divon M, Cornelius A, Rahav G, et al. A unique megaplasmid contributes to stress tolerance and pathogenicity of an emergent *S almonella enterica* serovar Infantis strain. Environ Microbiol 2014;16:977–94. https://doi.org/10.1111/1462-2920.12351.

[50] Gal-Mor O, Suez J, Elhadad D, Porwollik S, Leshem E, Valinsky L, et al. Molecular and cellular characterization of a Salmonella enterica serovar Paratyphi a outbreak strain and the human immune response to infection. Clin Vaccine Immunol 2012;19:146–56. https://doi.org/10.1128/CVI.05468-11.

[51] Bécavin C, Bouchier C, Lechat P, Archambaud C, Creno S, Gouin E, et al. Comparison of widely used Listeria monocytogenes strains EGD, 10403S, and EGD-e highlights genomic differences underlying variations in pathogenicity. MBio 2014;5. https://doi.org/10.1128/MBIO.00969-14/SUPPL_FILE/MBO002141775SD4.DOCX.

[52] Valdivia RH, Falkow S. Bacterial genetics by flow cytometry: rapid isolation of Salmonella typhimurium acid-inducible promoters by differential fluorescence induction n.d. https://doi.org/10.1046/j.1365-2958.1996.00120.x.

[53] Mambu J, Barilleau E, Fragnet-Trapp L, Le Vern Y, Olivier M, Sadrin G, et al. Rck of Salmonella Typhimurium Delays the Host Cell Cycle to Facilitate Bacterial Invasion. Front Cell Infect Microbiol 2020;10. https://doi.org/10.3389/FCIMB.2020.586934.

[54] Sanjana NE, Shalem O, Zhang F. Improved vectors and genome-wide libraries for CRISPR screening. Nat Methods 2014;11:783–4. https://doi.org/10.1038/NMETH.3047.

Figure Legends

Figure 1. CD81 surface expression in HepG2 cells facilitates invasion of various *Salmonella* serovars. (A) Flow cytometry staining profile of wild-type (*gray region*) and CD81-overexpressing HepG2 cells (*red region*). **(B)** Host association assay of *S.* Typhimurium SL1344; *S.* Enteritidis LA5, *S.* Infantis 119944 and *S.* Paratyphi A 45157 (MOI 10). The percentage of host-association (adherent and internalized bacteria) is calculated as a ratio of all associated bacteria with the host cells (30 min post-infection) normalized to the inoculum used for infection. **(C)** The percentage of invasion is calculated as a ratio of internalized bacteria recovered after gentamicin treatment (1.5 h p.i.), normalized to the inoculum. Data shown are mean +/- S.D. from a representative experiment of at least three independent experiments. **(D)** CD81-dependent host-association of *Salmonella* Typhimurium 14028s, S.Tm 14028s 3Δ mutant, and *rck*-complemented 3Δ mutant. The percentage of host-association (adherent and internalized bacteria) is calculated as a ratio of all associated bacteria with the host cells at MOI 10 (60 min post-infection) normalized to the initial inoculum and **(E)** percentage of invasion of *S.* Tm 14028s, *S.*Tm 14028s 3Δ mutant, and *rck*-complemented 3Δ mutant were calculated as a ratio of internalized bacteria recovered after gentamicin treatment (2.5 h p.i.) and cell lysis, normalized from initial inoculum used for infection. Data shown are mean +/- S.D. from a representative experiment of three independent experiments. **(F)** HepG2 cells (WT vs CD81-positive) were pretreated with HCV E2 for 1 h at 37°C, 5% CO_2 prior to gentamicin killing assay with *S.* Tm SL1344. Percent invasion is calculated as a ratio of the internalized bacteria recovered after cell lysis from total initial inoculum used for infection. Data shown are mean +/- S.D. from a representative experiment of two independent experiments. **(B-E)**: Data were analyzed using Student's t-test. ns, not significant, *P<0.05, **P <0.01, ***P<0.001, ***P<0.001, ****P<0.0001. **(F)**: Data were analyzed using one-way ANOVA followed by Tukey's post-hoc multiple comparison test. ns, not significant, *P<0.05, ****P<0.0001.

Figure 2. CD81-dependent *Salmonella* invasion is reduced by the lack of CD81 in C2BBe1 cells. (A) Flow cytometry staining profile of CD81-positive (*red region*) and CD81-knockout (*gray region*)

C2BBe1 cells. Adhesion and invasion assay of **(B-C)** *S.* Tm 14028, *S.*Tm 3Δ, *S.*Tm 3Δ+rck, and were analyzed for adhesion and invasion into C2BBe1 wt and CD81-deficient cells. Data shown are from a representative experiment of at least three independent experiments and were analyzed using Student's t-test. *P<0.05, **P<0.01, ***P<0.001, ns: not significant. **(D)** *L. monocytogenes* EGD invasion into C2BBe1 wt and CD81-deficient cells. Data are from one experiment and were analyzed using Student's t-test. *P<0.05). **(E)** Adhesion site of *S.* Tm SL1344 (MOI 100, green) on host cell surface showing cortical actin (*red*) and CD81 (*white*) and host nuclei (*blue*). Scale bar 20 µm. *Lower left panel*. Cropped and magnified image of adherent *S.* Tm on C2BBe1 cell surface. CD81 (*white, lower right panel*) is located mainly perinuclear / cytoplasmic with faint membrane staining. Actin cytoskeleton (*red, upper right panel*). Scale bar 5 µm. ROI = region of interest as indicated by the white frame in the overview panel. **(F)** Adhesion assay of *S.* Tm SL1344 (MOI 100, 60 min, 4°C). Data shown are from a representative experiment of three independent experiments and were analyzed using Student's t-test. ns: not significant. **(G)** Cell surface cholesterol depletion (with 10 mM methyl-ß-cyclodextrin, MßCD treatment for 15 min) impairs CD81-dependent *Salmonella* invasion in CD81-expressing C2BBe1 (MOI 10, 30 min). Internalized bacteria relative to the inoculum is reflected as percent invasion. Data shown are mean +/- S.D. from a representative experiment of two independent experiments and were analyzed using one-way ANOVA followed by Sidak's post-hoc multiple comparison test. ns, not significant, *P<0.05, ***P<0.001.

Figure 3. CD81 is recruited to actin-enriched membrane ruffles induced by *Salmonella* during invasion into C2BBe1 cells. (A) Imaging of C2BBe1 cells 15 min post-infection with GFP-expressing *S.*Tm SL1344 (*green*) at MOI 100. Magnified subsection is a membrane ruffle initiated by early invading salmonellae with CD81 recruitment (*white*) along an area with actin polymerization (*red*), nuclei shown in *blue*. Scale bar 20 µm. **(B)** Quantification of CD81 in *S.*Tm-induced ruffles: CD81 staining in *S.*Tm-induced ruffles were counted in eight FOV at 200X magnification and normalized to the total amount of infected cells. Data are mean +/- S.D. from a representative experiment of three independent experiments and were analyzed using one-way ANOVA followed by Tukey's post-hoc multiple comparison test. ns, not significant, ****P<0.0001.

Figure 4. CD81-mediated *Salmonella* invasion into epithelial cells is species-specific. (A) Flow cytometry staining histogram profiles of different HepG2 cell lines showing overexpression of human CD81 (*red*), rat CD81 (*blue*) and human CD9 (*green*). Wild-type HepG2 cells lack endogenous expression of CD81. **(B)** Overexpression of human CD81 but not rat CD81 facilitates invasion of *S.* Tm SL1344, 1.5 hours post-infection with an MOI of 10. Percent invasion is expressed as the ratio of internalized bacteria recovered after cell lysis to the inoculum used for infection. Data shown are mean +/- S.D. from a representative experiment of at least three independent experiments and were analyzed using one-way ANOVA followed by Tukey's post-hoc multiple comparison test. **P<0.01, ***P<0.001, ns: not significant. **(C)** Human CD9 localizes to *S.* Tm SL1344 (green) entry site during invasion. Human CD9 (*white*) is recruited along *S.* Tm SL1344 entry sites (*yellow arrows*) during early invasion of C2BBe1 cells, 15 min post-infection (MOI 100). *Upper right box inset*: overview of infected cells with enclosed region of interest. Scale bar 10 µm. **(D)** Adhesion assay of *S.* Tm SL1344 (MOI 100, 60 min, 4°C) in wild-type HepG2 cells and HepG2/hCD9. **(E)** Human CD9 overexpression facilitates *S.* Tm invasion in HepG2 cells but **(F-G)** CD9 does not affect host cell association or invasion into C2BBe1 cells. Data shown are mean +/- S.D. from a representative experiment of at least three independent experiments and were analyzed using a Student's t-test. ns: not significant, ***P<0.001.

Figure 5. CD81 and CD9 are recruited to the *Salmonella* entry site during invasion. **(A)** Immunostaining of human CD81 (*white, upper left panel*), human CD9 (*purple, upper right panel*), *S.* Tm SL1344 (*green*) and DAPI (*blue*) overlay (*lower left panel*) and merged frames (*lower right panel*) on C2BBe1 cells during early invasion of *S.* Tm SL1344 (15 min post-infection, MOI 100). Scale bar 5 µm. **(B)** Principle of *in situ* proximity ligation assay (PLA) detecting possible protein-protein interaction of CD81 and CD9 due to close proximity (~40 nm). Illustration created using Biorender.com **(C)** PLA signal (*red*) from CD9 and CD81 co-localization on host cell surface of C2BBe1 cells during early invasion of *S.* Tm SL1344 (*green*) validates their co-recruitment and

putative protein-protein interaction during *Salmonella* entry. Scale bar 5 µm (*upper right panel and bottom panels*). Overview of infected host cells (*upper left panel*) where nuclei are visible through DAPI staining (*blue*). Scale bar 20 µm.

Appendix. Supplementary data

Supplementary Figures

Figure S1. CD81-dependent *Salmonella* invasion is reduced by the lack of CD81 in HT29-MTX-E12 cells. (A) Anti-CD81 mAb treatment (*clear bars*) or IgG1 isotype matched mAb treatment (*shaded bars*) for 1 hour at 37°C, 5% CO_2 of HT29-MTX-E12 cells prior to infection with *S.* Tm SL1344. After 30 min of infection, cells were washed 3x with PBS and serial dilutions of cell lysates were plated to enumerate host-associated bacteria. **(B)** Flow cytometry staining profile of CD81-positive (*red region*) and, CD81-KO (*gray region*) HT29 MTX E12 cells after CRISPR/Cas9 targeting of CD81. **(C)** Gentamicin killing assay of HT29-MTX-E12 cells after infection with S. Tm SL1344 (MOI 10, 30 min). Percent invasion is calculated as a ratio of internalized bacteria recovered after cell lysis from initial inoculum used for infection. Data shown are mean +/- S.D. from a representative experiment of at least three independent experiments and were analyzed using a Student's t-test. ns, not significant, **P <0.01, ****P<0.0001.

Figure S2. CD81 staining of uninfected C2BBe1 cells: C2BBe1 were incubated at 37°C, fixed with PFA, permeabilised using 0.1% triton-X100 in 10% NGS/PBS. Anti-CD81 (white) antibody was diluted in blocking buffer containing the respective permeabilizing agents. After 3 washes secondary antibodies were applied. Cyotskeleton is stained using phalloidin (red) and nuclei were visualized using DAPI (blue). Note the typical perinuclear/cytoplasmic pattern of CD81 (green arrows) and membrane staining (yellow arrows). Scale bar: 20 µm.

Figure S3. MSA Alignment visualization of human CD81, rat CD81 and mouse CD81 using CLC sequence viewer 8.0.

Figure S4. CD9 localization in HepG2 cells. (A) HepG2 and HepG2/hCD9 cells were infected *S.* Tm SL1344 for 15 min. CD9 is weakly stained in HepG2 cells whereas there is a strong signal in HepG2/hCD9 cells. Human CD9 (*white*) partially recruited to *S.* Tm SL1344 entry sites (*yellow arrows*) and partially co-localized with actin. Scale bar: 10 µm. **(B)** Total RNA was extracted from uninfected HepG2 and HepG2/hCD9 cells. qPCR analysis of CD9 showed strong upregulation in CD9 overexpressing cells. CD9 overexpressing cells did not significantly induce CD81 expression. Data were analyzed using one-way ANOVA followed by Sidak's post-hoc multiple comparison test. ns, not significant, *P<0.05, ****P<0.0001.

Figure S5. Validation of *in situ* Proximity Ligation Assay of CD81/CD9 co-recruitment at the *Salmonella* entry site. Control set-ups (anti-CD81 only, anti-CD9 only or no antibodies) validating specificity of PLA signal to co-recruitment of CD9 and CD81 interaction during early invasion of *Salmonella* indicating its proximity and suggesting possible protein-protein interaction. Absence of, or addition of single antibodies targeting either CD9 and CD81 do not produce PLA signal. Scale bar: 20 µm. Illustrations created using Biorender.com.

[[Figure 1]]

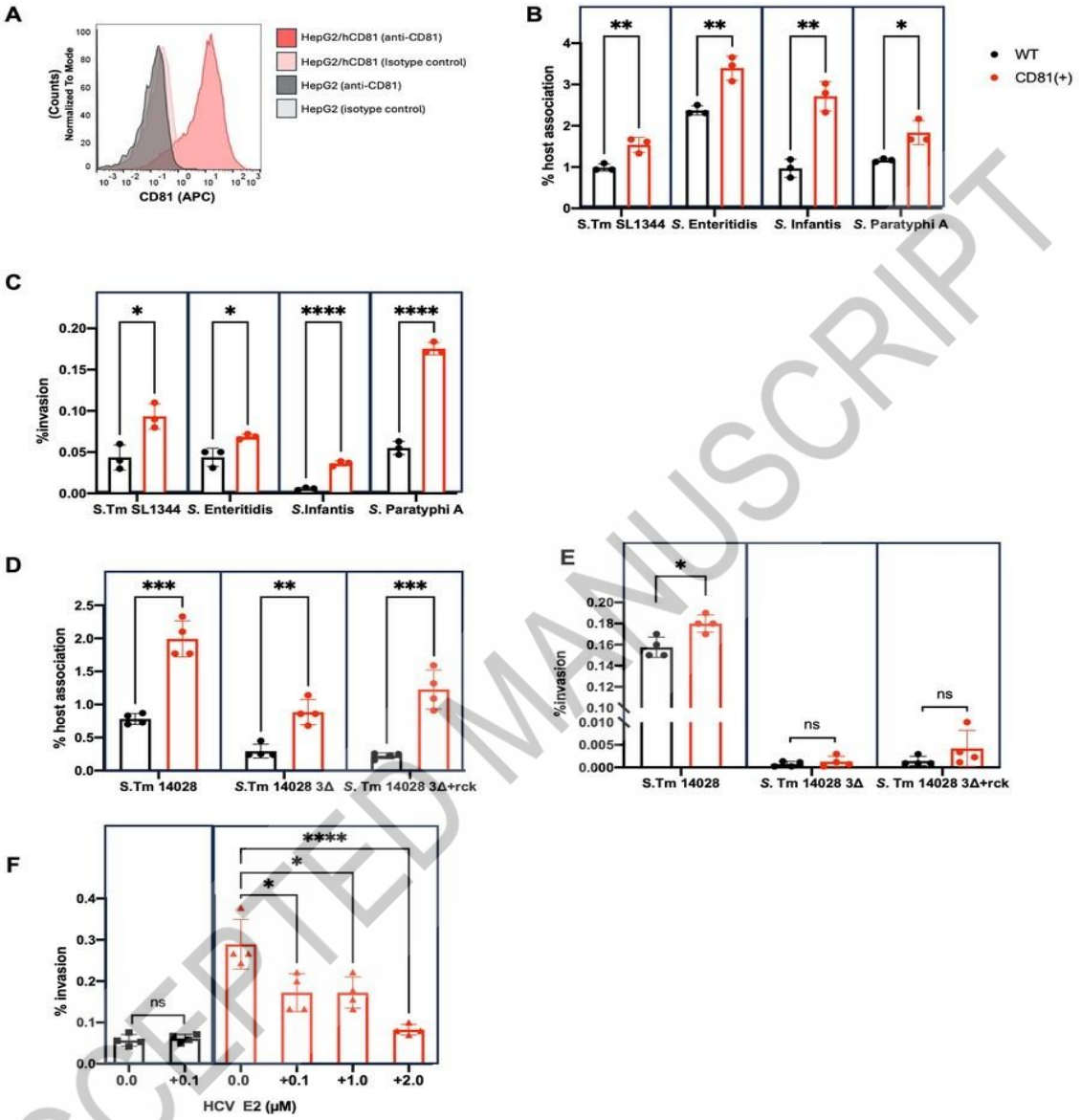

Figure 1 new

[[Figure 2]]

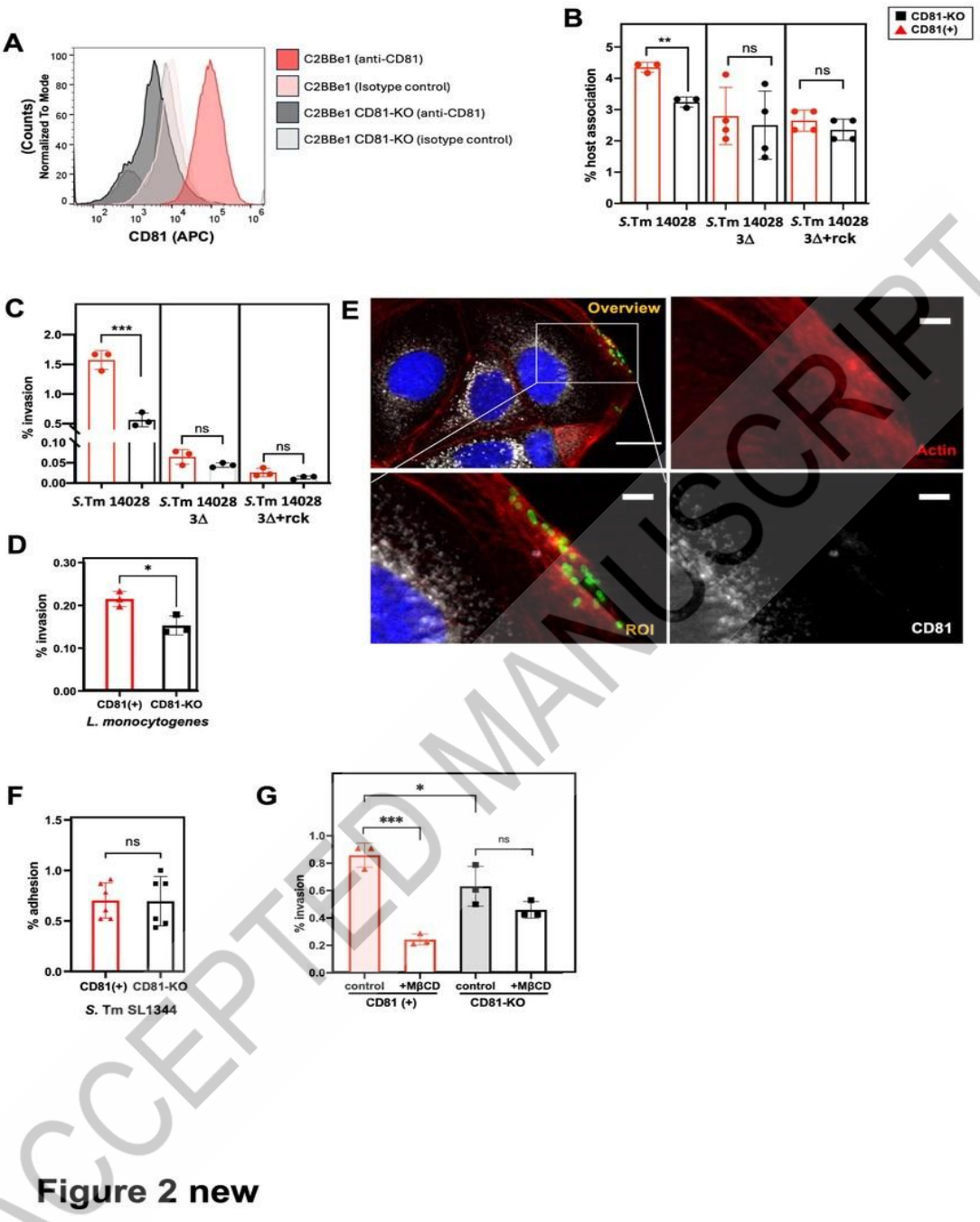

Figure 2 new

[[Figure 3]]

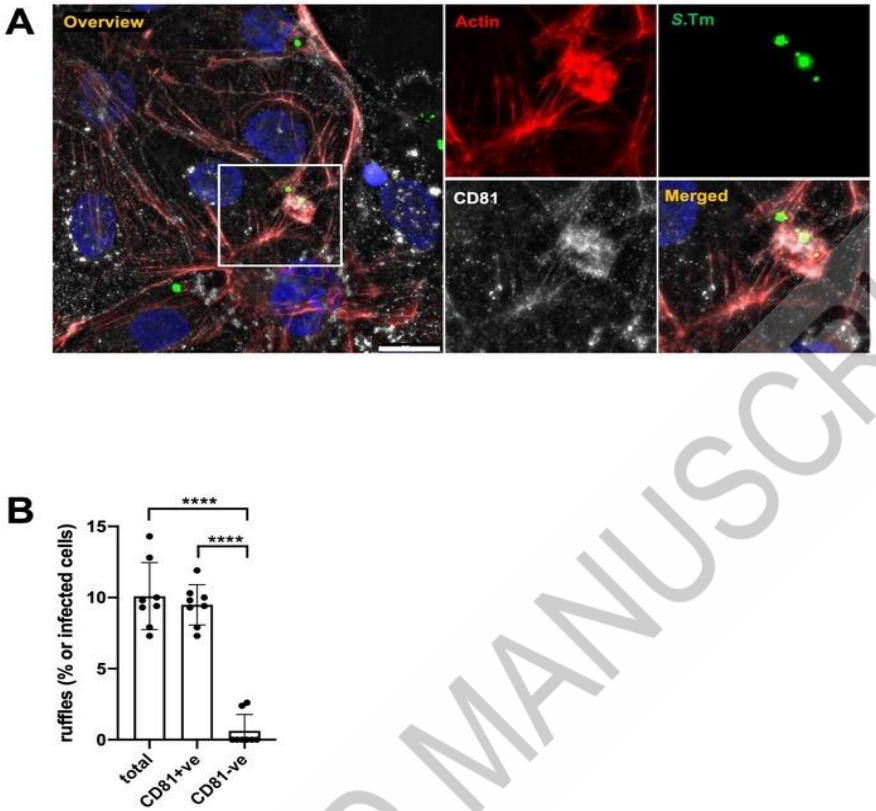

Figure 3 new

[[Figure 4]]

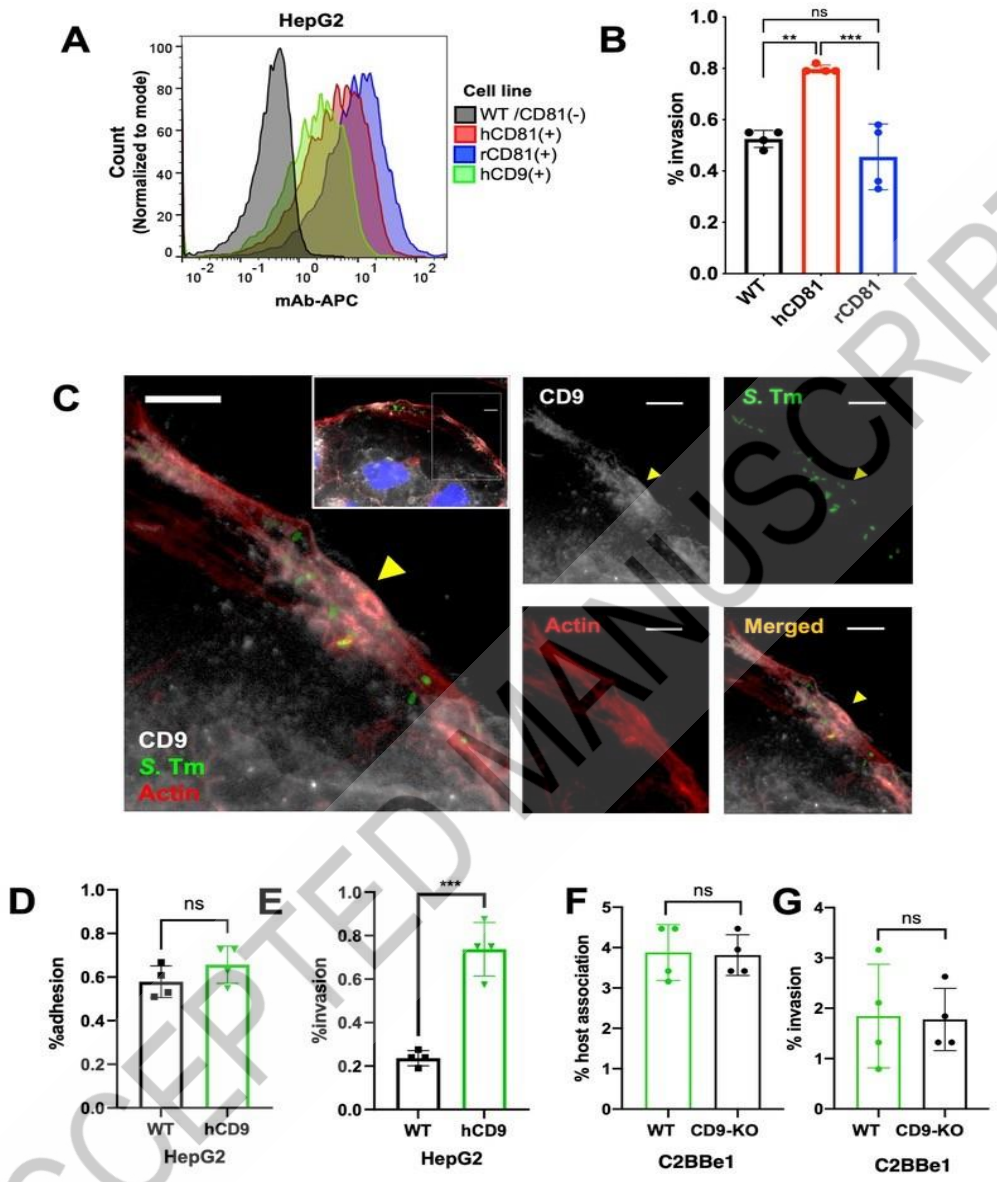

Figure 4

[[Figure 5]]

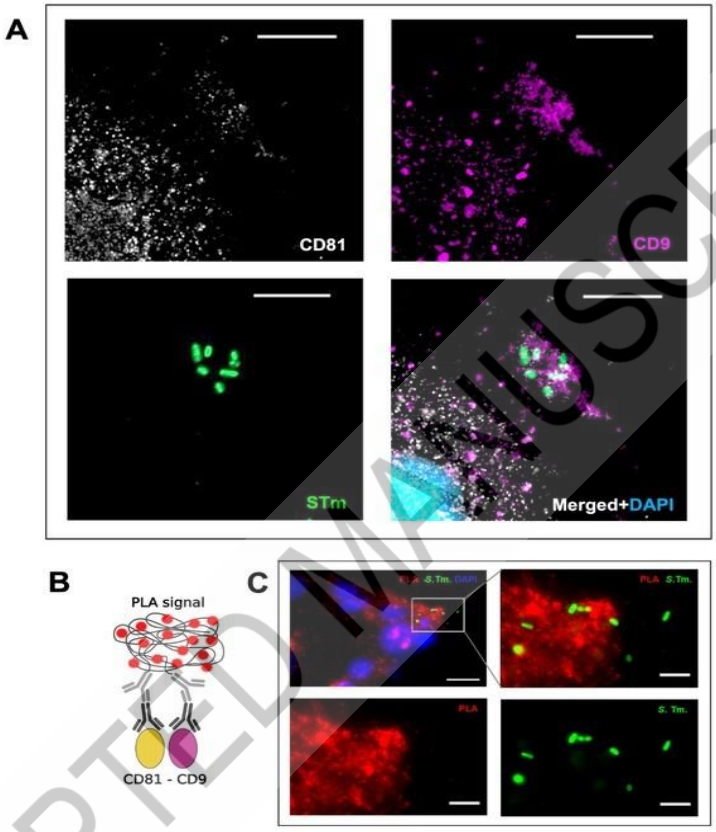

Figure 5

Table S1. List of Bacterial strains used in this study

Species	Serovar	Strain	Genotype	Plasmid	Resistance	Reference
Salmonella enterica	Typhimurium	SL1344	Wild-type	(-)	Streptomycin	[46]
Salmonella enterica	Typhimurium	14028s	Wild-type	(-)	None	[47]
Salmonella enterica	Enteritidis	LA5	Wild-type	(-)	Nalidixic Acid	[48]
Salmonella enterica	Infantis	119944	Wild-type	(-)	Tetracycline	[49]
Salmonella enterica	Paratyphi A	45157	Wild-type	(-)	No	[50]
Salmonella enterica	Typhimurium	14028s	3Δ *(ΔinvA::kanΔpagN::cm Δrck)*	(-)	Chloramphenicol Kanamycin	[26]
Salmonella enterica	Typhimurium	14028s	3Δ *(ΔinvA::kanΔpagN::cm Δrck)*	pSup202-GFP	Chloramphenicol Kanamycin Tetracyclin	This work
Salmonella enterica	Typhimurium	14028s	3Δ + *rck*	pSup202-RckGFP	Chloramphenicol Kanamycin Carbenicillin	This work
Listeria monocytogenes		EGD	Wild-type	(-)		[51]
Salmonella enterica	Typhimurium	SL1344	GFPmut3	pFPV25.1	Ampicillin	[52][52]

Table S2. List of plasmids

Plasmid name	Reference
pSup202-GFP	[53]
pSup202-RckGFP	[53]
pFPV25.1	[51]
pTRIP-hSEL-hLEL CD81 (human CD81)	[35]
pTRIP-rSEL-rLEL CD81 (rat CD81)	[35]
pTRIP-human CD9	[35]
pczVSV-Gwt	[12]
pCMV-dR8.74 GK	[12]
pLentiCRISPR V2	[54]
pLentiCRISPR V2-CD81	[12]
pCMV-dR8.74 GK	[12]

Table S3. List of antibodies used for flow cytometry and Fluorescence Activated Cell Sorting

Target	Clone	Fluorophore	Brand	Catalog no.	RRID no.
Human CD81	JS-81 RUO	APC	BD Bioscience	551112	AB_398491
IgG1-Kappa	MOPC-21	APC	BD Bioscience	555751	AB_398467
Human CD81	5A6	APC	Biolegend	349509	AB_2564020
Human CD9	Hl9a-RUO	APC	Biolegend	312107	AB_2721450
IgG1-Kappa Isotype	MOPC-21	APC	Biolegend	400121	AB_2665396
Rat/mouse CD81	Eat-2	APC	Biolegend	104909	AB_2562993
IgG1-Kappa isotype	HTK888	APC	Biolegend	400911	(-)

Table S4. List of Primary Antibodies used for immunofluorescence, blocking and PLA experiments

Target/ Reactivity	Clone	Host	Brand	Catalog no.	RRID no.
Human CD81	JS-81 RUO	Mouse	BD Bioscience	555675	AB_396028
IgG1 isotype cntrl	MOPC-21	mouse	BD Bioscience	555746	AB_396088
Human CD81	NA	Rabbit	Invitrogen	PA5-82288	AB_2789447
Human CD9	Hl9a-RUO	mouse	Biolegend	312102	AB_314907

Table S5. List of Secondary Antibodies used for immunofluorescence

Reactivity	Fluorophore	Brand	Catalog no.	RRID no.
anti-rabbit	Alexa Fluor®546	Invitrogen	A-11071	AB_2534115
anti-mouse	AlexaFluor®633	Invitrogen	A-21050	AB_2535718
anti-mouse	AlexaFluor®546	Invitrogen	A-11003	AB_2534071
anti-mouse	AlexaFluor®633	Invitrogen	A21053	AB_2535720
anti-rabbit	AlexaFluor®633	Invitrogen	A21072	AB_2535733

Table S6: Percent identity matrix of the aligned CD proteins (Clustal).

Tetraspanin	human CD81	mouse CD81	rat CD81
human CD81	100.00	91.95	93.22
mouse CD81	91.95	100.00	94.49
rat CD81	93.22	94.49	100.00

[[Supplementary Figure 1]]

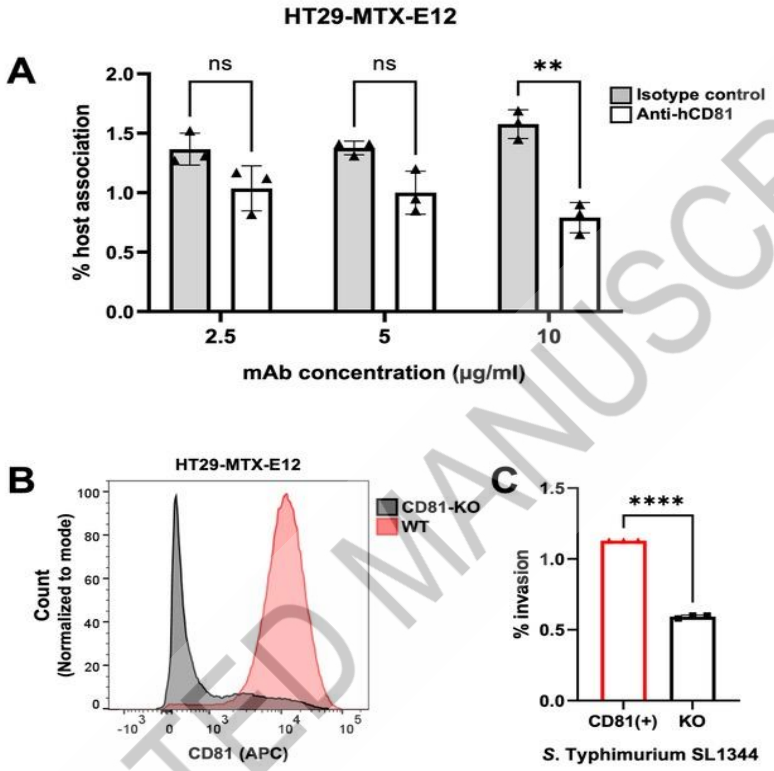

Figure S1

[[Supplementary Figure 2]]

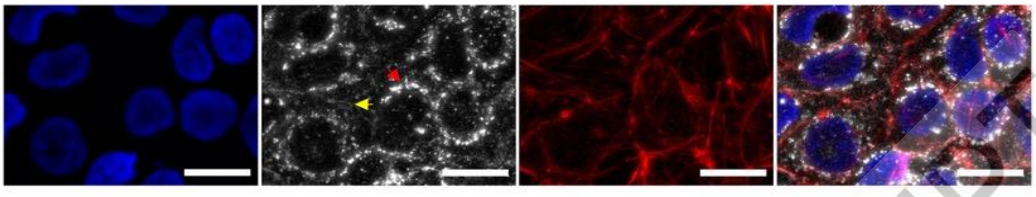

Figure S2

[[Supplementary Figure 3]]

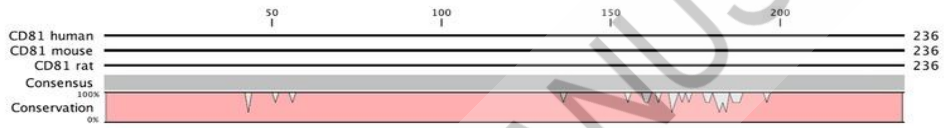

Figure S3

[[Supplementary Figure 4]]

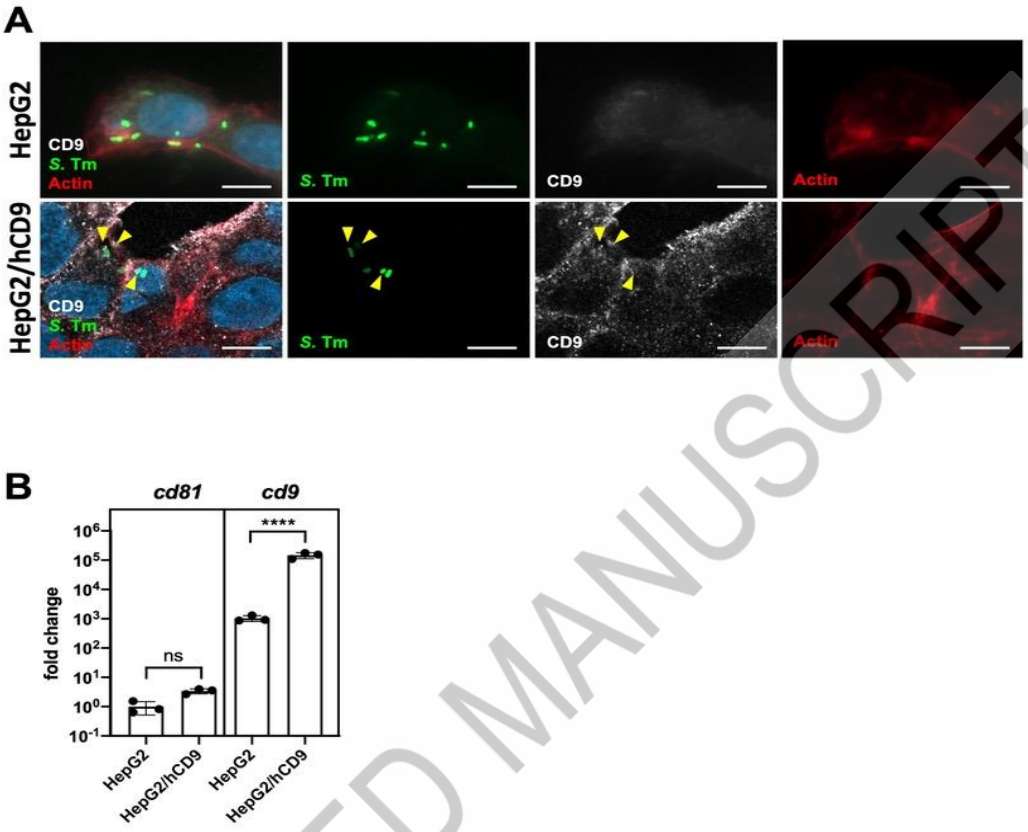

Figure S4 new

[[Supplementary Figure 5]]

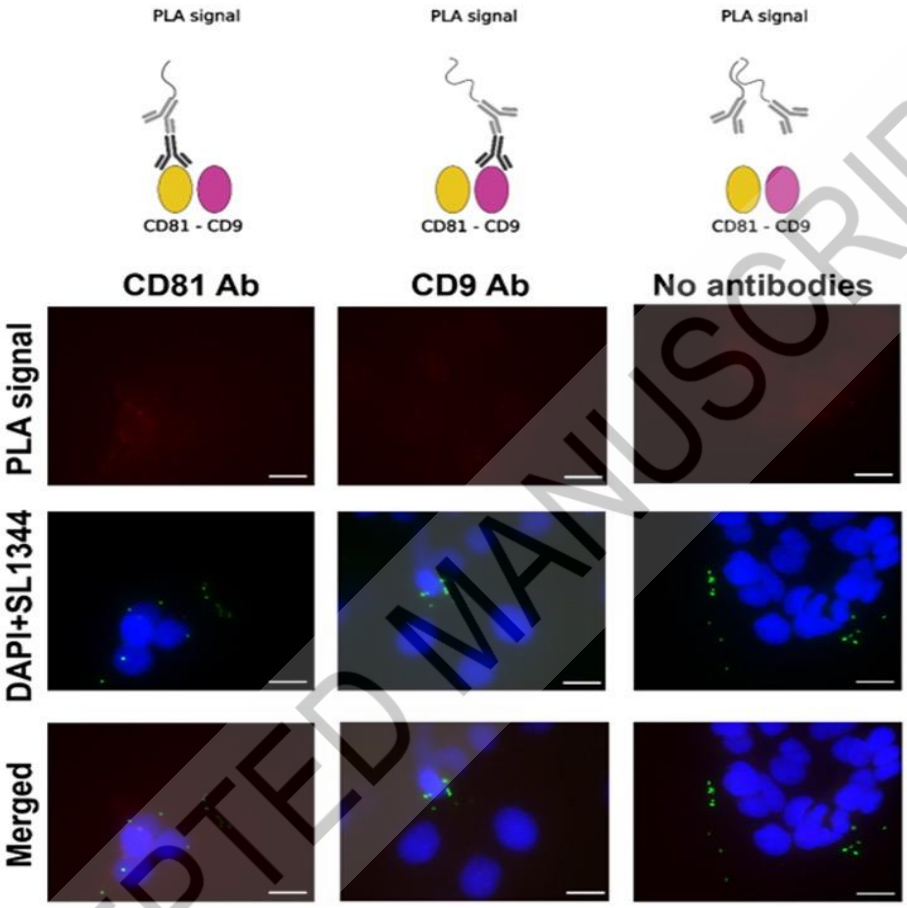

Figure S5 new